MODELLING SIMULTANEOUS NITRITATION AND *p*-NITROPHENOL REMOVAL USING AEROBIC GRANULAR BIOMASS IN A CONTINUOUS AIRLIFT REACTOR

SITI FITRIANA ALANG AHMAT

BACHELOR OF CHEMICAL ENGINEERING
UNIVERSITI MALAYSIA PAHANG

Thesis Access Form

No_____Location_____

Author : ……

Title : ……

Status of access OPEN / RESTRICTED / CONFIDENTIAL

Moratorium period:_____ years, ending_____/_____200____

Conditions of access proved by (CAPITALS): DR ZULKIFLY BIN JEMAAT

Supervisor (Signature)……

Faculty: ……

Author's Declaration: *I agree the following conditions:*

OPEN access work shall be made available (in the University and externally) and reproduced as necessary at the discretion of the University Librarian or Head of Department. It may also be copied by the British Library in microfilm or other form for supply to requesting libraries or individuals, subject to an indication of intended use for non-publishing purposes in the following form, placed on the copy and on any covering document or label.

*The statement itself shall apply to **ALL** copies:*

This copy has been supplied on the understanding that it is copyright material and that no quotation from the thesis may be published without proper acknowledgement.

Restricted/confidential work: All access and any photocopying shall be strictly subject to written permission from the University Head of Department and any external sponsor, if any.

Author's signature…….Date: ……

users declaration: for signature during any Moratorium period (Not Open work): ***I undertake to uphold the above conditions:***			
Date	Name (CAPITALS)	Signature	Address

MODELLING SIMULTANEOUS NITRITATION AND *p*-NITROPHENOL REMOVAL USING AEROBIC GRANULAR BIOMASS IN A CONTINUOUS AIRLIFT REACTOR

SITI FITRIANA ALANG AHMAT

Thesis submitted in partial fulfilment of the requirements
for the award of the degree of
Bachelor of Chemical Engineering

Faculty of Chemical & Natural Resources Engineering
UNIVERSITI MALAYSIA PAHANG

JANUARY 2015

SUPERVISOR'S DECLARATION

We hereby declare that we have checked this thesis and in our opinion, this thesis is adequate in terms of scope and quality for the award of the degree of Bachelor of Chemical Engineering.

Signature :
Name of main supervisor : DR. ZULKIFLY BIN JEMAAT
Position : SENIOR LECTURER
Date : 12 JANUARY 2015

STUDENT'S DECLARATION

I hereby declare that the work in this thesis is my own except for quotations and summaries which have been duly acknowledged. The thesis has not been accepted for any degree and is not concurrently submitted for award of other degree.

Signature :
Name : SITI FITRIANA BINTI ALANG AHMAT
ID Number : KA11041
Date : 12 JANUARY 2015

DEDICATION

To my helpful supervisor, parents, and friends

ACKNOWLEDGEMENT

I am grateful and would like to express my sincere appreciation to my main thesis supervisor, Dr. Zulkifly Bin Jemaat for his germinal ideas, invaluable guidance, continuous encouragement and constant support in making this research possible. He has always impressed me with his outstanding professional conduct, his strong conviction for science, and his belief that a bachelor program is only a start of a lifelong learning experience. Without his continuous support and interest, I would not have been able to complete this final year project successfully. I also sincerely thanks for the time spent proofreading and correcting my many mistakes.

I am also indebted to Universiti Malaysia Pahang (UMP) for providing internet and final year project lab facility. Special thanks also given to librarians UMP for their assistance in supplying the relevant literatures and are useful indeed. I acknowledge my sincere indebtedness and gratitude to my parents for their love, dream and sacrifice throughout my life. I am also grateful to my fellow members for their supportive and helps that were inevitable to make this work possible. I cannot find the appropriate words that could properly describe my appreciation for their devotion, support and faith in my ability to attain my goals. I would like to acknowledge their comments and suggestions, which was crucial for the successful completion of this study.

ABSTRACT

A mathematical biofilm model was developed with a dual-biomass kinetic including Haldane formalism to describe simultaneous nitritation and p-nitrophenol (PNP) removal in aerobic granular biomass operating in continuous airlift reactor. The model was validated with a set of experimental result previously reported in the literature. Then, the model was explored further to study the influence of pH, initial concentration of PNP in the influent, temperature of the operating system, and the influent loading rate for total ammonia nitrogen (TAN) and p-nitrophenol. The result showed that the maximum capacity of the reactor to treat simultaneous nitritation and PNP were 46.15 gN $L^{-1}d^{-1}$ and 288.5 mg PNP $L^{-1}d^{-1}$, respectively. Studying the effect of pH value in simultaneous nitritation and PNP removal, it showed that the range for optimum operation is between 7.3 and 8.3. While, the maximum advisable operating temperature is at 55°C. Higher operating temperature would result to a poor removal performance. In conclusion, simultaneous nitritation and PNP removal could be achieved in a single rector by using granular biomass.

ABSTRAK

Model biofilm matematik telah digunakan dengan kinetik dwi-biomas termasuk Haldane formalisme untuk menggambarkan nitritation serentak dan p-nitrophenol (PNP) penyingkiran dalam aerobik berbutir biomass yang beroperasi di reaktor pengangkutan udara berterusan. Model ini telah disahkan dengan satu set hasil eksperimen yang dilaporkan sebelum ini dalam kesusasteraan. Kemudian, model ini telah diterokai lagi untuk mengkaji pengaruh pH, kepekatan awal PNP dalam influen, suhu sistem operasi, dan kadar beban influen untuk jumlah ammonia nitrogen (TAN) dan p-nitrophenol. Hasilnya menunjukkan bahawa kapasiti maksimum reaktor untuk merawat nitritation serentak dan PNP adalah 46,15 gN $L^{-1}d^{-1}$ dan 288,5 mg PNP $L^{-1}d^{-1}$. Mengkaji kesan nilai pH dalam nitritation serentak dan penyingkiran PNP, ia menunjukkan bahawa julat bagi operasi optimum adalah antara 7.3 dan 8.3. Di samping itu, suhu operasi maksimum adalah pada 55 ° C. Suhu operasi yang lebih tinggi akan menyebabkan prestasi penyingkiran yang lemah. Kesimpulannya, nitritation serentak dan penyingkiran PNP boleh dicapai dalam rektor tunggal dengan menggunakan biomass berbutir.

TABLE OF CONTENTS

LIST OF FIGURES

LIST OF TABLES

LIST OF ABBREVIATIONS

b_{AER}	Aerobic decay rate
b_{ANAER}	Anaerobic decay rate
b_{PNP}	PNP decay rate
b_H	Heterotrophic decay rate
K	Affinity constant
K_I	Inhibition Coefficient
S	concentration
Y	Growth yield

Greek word

µmax	Maximum Specific growth rate

LIST OF ABBREVIATIONS

ALR	Air-lift reactor
AOB	Ammonia oxidizing bacteria
BT	Benzenetriol
DO	Dissolve oxygen
EPA	Environmental Protection Agency
FA	Free ammonia
FNA	Free nitrous acid
HRT	Hydraulic retention time
NOB	Nitrite oxidizing bacteria
PNP	*p*-nitrophenol
SBR	Sequencing batch reactor
TAN	Total ammonia nitrogen
TNN	Total
WHO	World Health Organization

1 INTRODUCTION

1.1 Background of study

Aerobic granulation, a novel environmental biotechnological process, is increasingly drawing interest of researchers engaging in work in the area of biological wastewater treatment (Adav et al.,2008 ; Lee et al,2010; Adav et al.,2009) due to the limitation of current biological wastewater treatment (activated sludge). Aerobic granules technology has been reported in treating a vast pollutant constitutes such as high strength organic wastewaters, toxic aromatic pollutants such as phenol, toluene, dinitrotoluene, pyridine and textile dyes, removal of nitrogen, phosphate and sulphate, adsorption of heavy metals and nuclear waste.(Mascolo et al.,2010; Adav et al.,2009; Jemaat et al.,2013a; Reddy et al.,2014;). In addition, aerobic granular biomass are known to perform better in front of inhibitory or toxic compound compared to activated sludge system because granule architecture causes diffusion gradients contributing to protect sensitive bacteria (Adav et al.,2009; Maszenan et al.,2011). Frequently chemical and petrochemical industries produce complex industrial wastewater containing nutrients and toxic compounds. Nutrients could be easily handled by biological treatment, but toxic compounds in the wastewater need an extra caution to be treated. Commonly, conventional biological treatment is operated in batch reactors. However, this operation is not suitable for treatment of phenolic compounds that habitually demonstrate inhibition by substrate (Martín-Hernández et al, 2009). Therefore, continuous operation might be a proper option, as the concentration of the recalcitrant compounds in the reactor is estimated to be low due to the great removal efficiency, decreasing their toxic effect in the reactor. This great removal efficiency might be achieved from the starting of the operation by execution a controlled enrichment of the specific degrading biomass, i.e. by feeding this kind of compounds gradually in the start-up (Jemaat et al,2013a). In the case of wastewater containing ammonia and PNP,to keep the condition in which simultaneous nitritation and p-nitrophenol removal is stable, keeping under control the ammonium and p-nitrophenol (PNP) concentration in the effluent would be also desirable, since the potential inhibition of ammonium oxidising bacteria (AOB) and nitrite oxidising bacteria (NOB) by PNP will be easily handled, which must be accounted for in the modelling of pollutant mass transfer and reaction.

In this study, an attempt has been made to use a biofilm modelling approach to reproduce the simultaneous nitritation and p-nitrophenol (PNP) removal in aerobic granular biomass. The model includes the growth of five microbial groups (ammonia-oxidizing bacteria (AOB), nitrite-oxidizing bacteria (NOB), p-nitrophenol degrader, heterotrophic bacteria, and inert biomass) operated in continuous airlift reactor. The processes occurring in the biofilms are simulated in the one-dimensional (1-D) mathematical biofilm model of the simulator AQUASIM (Reichert,1998), a programme for identification and simulation of aquatic systems. For the rate equations and kinetics of the microbiological processes, the dual-biomass kinetic including Haldane formalism of bio kinetic model as described in Jubany et al.(2008), Munz et al.(2011), Tziotzios et al, (2008) and general equation for heterotrophic decay rate were used. The results are compared and contrasted with those in the work of Jemaat et al. (2013a) who successfully demonstrated simultaneous nitritation and PNP removal in an airlift biofilm reactor .Then, the model was explored further to study the influence of pH, initial concentration of PNP in the influent, temperature of the operating system and the influent loading rate for total ammonia nitrogen (TAN) and PNP. Although biofilm modelling may represent a theoretical improvement over the "suspended bacteria" approach in constructed aerobic granular biomass modelling, a direct comparison of the modelling approaches and the experimental study is important to determine if the biofilm modelling approach yields new qualitative information, specifically on the possible influence of the boundary conditions of temperature and microbial species on the prediction of substrate removal in constructed aerobic granular biomass.

1.2 Motivation and statement of problem

In practice, during the experimental works only one or two parameters can be manipulated to achieve a specific objective. Once the desired parameter is adjusted, the researcher or operator needs to wait until the system reaches a steady state condition before the action of manipulating a new parameter could take place. Achieving a steady state condition while manipulating any process variable is very important to observe closely the response of the system towards the changes made. Depending on the nature of the experiment, to achieve a steady state condition it is time consuming i.e it can take a few days up to months. Imagine if the research has a long list of process variables that need to be studied at a very limited time. By using a simulation study, this drawback could be solved and save time provided the developed model is properly validated, calibrated and tested according to the real experiment

data collected. Simulation study is also a very useful tool in the industrial process practice due to the nature of operation (non-stop) and predicting process behaviour when certain process parameters need to be changed. In other words, by conducting simulation study, prediction of the process behaviour can be obtained in a fast time and overcome the limitation of experimental works.

1.3 Objective

The objective of this research is to develop a model for study the simultaneous biological removal of industrial wastewater containing ammonium and phenolic compound

1.3.1 Scope of this research

In order to achieve the objective of this research, few scopes have been identified and will be covered:

i) Developing a model that has a good correlation with existing experimental data obtained by Jemaat et al, 2013.

ii) Validate, calibrate and fine tune the developed model to achieve good prediction with experimenter data obtain by Jemaat et al, 2013.

iii) Studying, explore and analysing the model simulation with several scenarios related to operational variability faced by certain industries (i.e temperature, inflow characteristic, concentration and pH value)

2 LITERATURE REVIEW

2.1 Aerobic granular biomass

Aerobic granulation is a complex practice affected or regulated by numerous factors and primarily dependent on reactor configuration, environmental and operating conditions. The operational parameters comprising substrate loading rate, aeration intensity, feast–famine regime, settling time and hydraulic retention time (HRT) may be manipulated within the laboratory scale granulation SBR to energetically pick for stable aerobic granular sludge development. Findings have proved that an appropriate HRT should be sensibly picked and gently upheld for optimization of the reactor operation. (Rosman et al, 2014).Compared to activated sludge, granules has advance settling ability, greater density, robust microbial structure, higher biomass retention and well nutrient removing capability. More freshly, the sequencing batch reactor has been operated to research granulation under aerobic circumstances (Rocktäschel et al., 2013; Zhang et al., 2011). Failure of granule stability is a main obstacle to applied applications for long-standing process and several researches have shown that aerobic granules would disintegrate after protracted process (Tay et al, 2011; Jiang et al., 2002). Thus, an advancement of the permanency of aerobic granular sludge and an extension of service life of aerobic granules are required, which would have a key effect on the wastewater treatment (Liu et al, 2014)

The aerobic granular sludge process is a talented technology for wastewater treatment since it could reduce the financing and operating budgets as well as space necessities (Liu et al., 2010; Zhu et al., 2013). Besides, it has the ability to achieve an effective removal of nutrients in a single reactor, because the nitrification, denitrification and biological P removal could be carried out within the granules (de Kreuk et al., 2005; Coma et al.,2012; Di Bella and Torregrossa, 2013; Li et al,2014)

2.2 Air-lift Reactor

An air-lift is a modified bubble column reactor described by three different parts namely *riser, gas–liquid separator,* and *downcomer*. The driving force in air-lift reactors is the gas injection which stimulates the liquid circulation (Cockx et al. 1997) .Liquid circulation is stimulated through introducing gas at the base of the riser, hence forming a clear density difference between riser and downcomer (Camarasa et al, 2001). Air-lift reactor (ALR) has been known as an cost-effectively and technically important option with straightforward design and construction, great competence of homogenization and intense mixing for heat and mass transfer, low power consumption, and shear stresses(Jin et al, 2006). The ALRs are predominantly appropriate for a process which stresses prompt and uniform distribution of the reaction components, and for multiphase (gas–liquid–solids) systems in which high mass and heat transfer are compulsory , and have been extensively utilized in biochemical industry, fermentation and biological wastewater treatment processes (Jin et al, 2006) . Figure 1 below shows a laboratory scaled of an airlift reactor used by Jemaat et al.,(2013a).

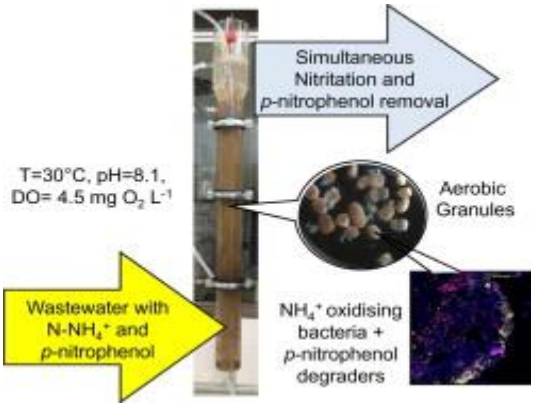

Figure 1 Air-Lift Reactor and Aerobic Granules (Jemaat et al, 2013)

For design, operation and control intentions, an exact simulation of the reactor operation is vital. The model must comprise mass transfer, reaction kinetics, flow configuration and hydrodynamics. However, modelling of reactions in air-lift reactors is quiet problematic mostly because the reactor hydrodynamic complexity is rose by the non-coalescing actions of the organic liquid mixture faced in industrial reactors. An effective assumption of hydrodynamics parameters (the gas hold-up and the liquid circulation velocity) can be done with a great model created both on a precise equations system and on experimental results.(

E. Camarasa et al,2001). Furthermore, the modelling of air-lift reactor can be attained at various levels equivalent to diverse approaches of the problem. (Cockx et al., 1997)

2.3 P-Nitrophenol

p-Nitrophenol (PNP) is a synthetic chemical that is generally consumed as a starting material for production of drugs, fungicides, insecticides, dyes and to darken leather (Guo et al, 2014). PNP is one of the greatest consumed nitro phenolic compounds in the industry, being comprised in the record of High Volume Production Chemicals by the Organization for Economic Cooperation and Development which proposes to manufactured in quantities more than 1000 ton/year in as a minimum one member/country (Martín-Hernández et al, 2012). The specific nomenclature of this substance is 1-hydroxy-4-nitrobenzene and it is more likely known as p-nitrophenol or 4-nitrophenol (Lide, 2002a). It has two constitutional isomers, namely, o-nitrophenol (2-nitrophenol) and m-nitrophenol (3-nitrophenol). They share the same empirical formula of C6H5NO3. The structural formulas are shown in figure 2.

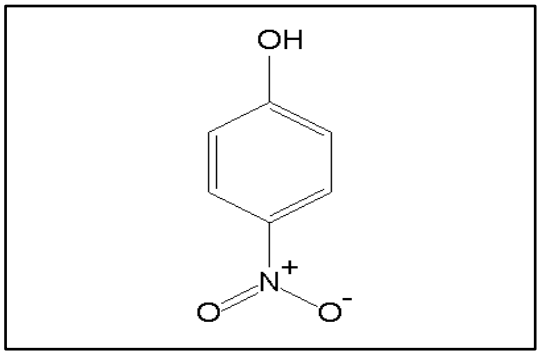

Figure 2: Molecular structure for p-Nitrophenol (Janice Gorzynski Smith, 2011)

PNP forms colorless to slightly yellow odorless crystals at room temperature with sweetish, then burning taste (O'neil et al., 2001). The physical and chemical properties of the substance are shown in Table 1.

Table 1 Properties of *p*-Nitrophenol

Properties of *p*-Nitrophenol

Molecular formula	$C_6H_5NO_3$
Molar mass	139.11 g/mol
Appearance	Colourless or yellow pillars
Melting point	113 to 114 °C (235 to 237°F)
Boiling point	279 °C (534°F,552 K)
Solubility in water	10 g/L (15 °C) 11.6 g/L (20 °C) 16 g/L (25 °C)

Due to the extensive use of *p*-Nitrophenol (PNP) in agronomy and manufacturing sectors, PNP broadly exist in agricultural irrigation flows and industrial effluents . The existence of a nitro-group in the aromatic ring of PNP lead to several harmful characteristics, such as toxicity, non-biodegradation and excessive persistence in the environment, so it has been judged to be the precedence toxic pollutant by U.S. Environmental Protection Agency (EPA) and the usage of PNP is no longer advocated corresponding to the Standards for Chemical Products in UK (Wang et al, 2014).

PNP is extremely toxic for humans and environment; repetitive contact may cause damage to blood cells, harm to the central nervous system and mutagenic effects. Furthermore, a research carried out about the European rivers quality proved that PNP was exist in 97% of the studied samples from over 100 rivers tested (Martín-Hernández et al, 2012).Table 1 below shows the properties of p-nitrophenol.

Various PNP-degrading bacteria have been isolated, and their degradation characteristics have been comprehensively reviewed (Spain et al.,2000; Lynda and Zylstra,2007). PNP be able to aerobically degraded by two dissimilar routes. In the meta-cleavage routes,

preferentially establish in gram-positive bacteria such as *Bacillus* spp. (Jain et al.,1994) and *Arthrobacter* sp (Kadiyala and Spain.,1998), degradation of PNP arises through the formation of benzenetriol , (BT) (Shen et al,2010).

In biological practices degrading phenols, substrate inhibition is one of the more often experimental mechanisms, which has been extensively reviewed and modelled with the Haldane formalism (Haldane,1996, Grady and Lim,1980, Rozich et al,1985, Meric et al., 2002 and Saravanan et al.,2008). The biodegradation of nitrophenol in pure cultures has been examined (Simpson and Evans,1953; Zeyer and Kearney, 1984; Lenke et al.,1992 and Löser et al,1998). Species as *Bacillus sphaericus* (Kadiyala et al.,1998),*Pseudomonas putida* (Kulkarni and Caudhari,2006), *Rhodococcus wratislaviensis* (Gemini et al.,2005) were skilled to degrade PNP.(Tomei et al., 2006) isolated a gram negative coccobacillum member of *Ralstonia* genus within *Betaproteobacteria* able to grow aerobically on *p* -NP as the sole carbon supply in the range of 80–320 mg l^{-1}. These had exposed the biodegradability of *p*-NP and proved the substrate inhibition of the microorganism action depending on the culture environments (Rezouga et al, 2009)

2.4 Ammonia

Ammonium is a toxic chemical that has turned out to be a main environmental pollutant (Yu et al, 2012). Ammonium together with its oxidation products (i.e. nitrate), extensively dispersed in the industrial and domestic waste water, can readily trigger eutrophication and therefore affect ecosystem and human health.(Shi et al, 2013). Drinking water containing excessive nitrate can cause cancer and other diseases. According to WHO, the amount of nitrate in drinking water should not be more than 50 mg L^{-1} and European Community recommends levels of 25 mg L^{-1}.So it is compulsory to decrease nitrate concentration before discharging. Figure 3 below shows the molecular structure for ammonia.

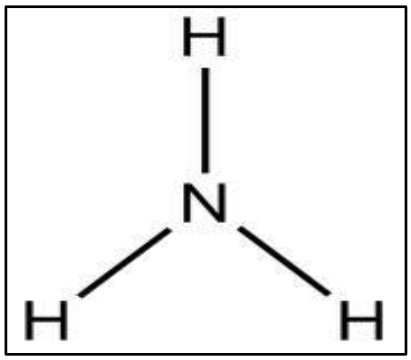

Figure 3: Molecular structure for Ammonia (Janice Gorzynski Smith, 2011)

The recovery and removal of NH_4–N can be done by biological, physical, chemical, or a combination of these methods. Existing technologies comprise adsorption, chemical precipitation, membrane filtration, reverse osmosis, ion exchange, air stripping, breakpoint chlorination and biological nitrification and denitrification (Wahab et al, 2010). The biological removal of nitrogen has been identified as the principal method in terms of cost, removal efficiencies and implementation. Ammonium removal by heterotrophic microorganisms has commonly been reported to oxidize NH_4^+-N to NO_2^--N or NO_3^--N and simultaneously covert NO_2^--N or NO_3^--N to N_2O and/or N_2 (Zhang et al, 2013). Earlier findings stated that heterotrophic bacteria could remove ammonium at low temperature (Zhang et al.,2011). Because heterotrophic microorganisms often require high concentrations of ammonium and organic carbon (ammonium above 50 mg/L and *C*/*N* above 8), they are usually consumed in wastewater treatment (Zhang et al, 2013). For more information, Table 2 below shows selected properties of ammonia

Table 2 Properties of Ammonia (Janice Gorzynski Smith, 2011)

Properties of Ammonia	
Molecular formula	NH_3
Molar mass	17.031 g/mol
Appearance	Colourless gas
Odour	Strong pungent odour
Density	0.86 kg/m^3(1.013 bar at boiling point)
	0.769 kg/m^3(STP)
	0.73 kg/m^3(1.013 bar at 15°C)
	681.9 kg/m^3 at -33.3°C (liquid)
	817 kg/m^3 at -80°C (transparent solid)
Melting point	-77.73°C (-107.91°F,195.42K)
Boiling point	-33.34°C (-28.01°F,239.81K)
Solubility	Soluble in chloroform, ether, ethanol, methanol
Acidity(pKa)	32.5(-33 °C)
Basicity (pKa)	4.75

2.5 AQUASIM Software

AQUASIM is a computer program for the identification and simulation of aquatic systems. The program comprises a one-dimensional multi-substrate and multispecies biofilm model and signifies an appropriate tool for biofilm simulation. The program can be operated to compute substrate elimination in biofilm reactors for any manipulator specified microbial system. One-dimensional spatial profiles of substrates and microbial species in the biofilm can be predicted. The program also computes the progress of the biofilm thickness and of the substrates and microbial species in the biofilm and in the bulk fluid over time. Detachment and attachment of microbial cells at the biofilm surface and in the biofilm interior can be judged, and simulations of sloughing actions can be operated. The mainly significant

drawback of the model is that it merely reflects spatial gradients of substrates and microbial species in the biofilm in the way perpendicular to the substratum. (Reichert, 1998)

2.5.1 Feature of the biofilm model implemented in AQUASIM

2.5.1.1 The biofilm reactor compartment

For biofilm modelling and simulation, AQUASIM recommends a biofilm reactor compartment comprising of three zones: “bulk fluid,” “biofilm solid matrix,” and “biofilm pore water”. For all three zones, AQUASIM analyses the development over time of microbial species and substrates, along with the biofilm thickness. In the biofilm, spatial slopes perpendicular to the substratum are considered for microbial species and substrates. The bulk fluid is expected to be completely mixed, and a liquid boundary layer between the Water Science and Technology Vol 49 No 11–12 pp 137–144 © IWA Publishing 2004 137 biofilm and the bulk fluid can be counted. The AQUASIM biofilm reactor compartment can be linked to other compartments.

In the AQUASIM dialog box “Edit Biofilm Reactor Compartment” (Figure 1), the properties of the biofilm system to be developed are detailed. The reactor type is selected to be “confined” if the volume of the biofilm as well as the bulk fluid is constant, the way it is a closed reactor, and to be “unconfined” if the biofilm be able to grow up freely, as may be the case in a trickling filter. The pore volume can be indicated to enclose only a liquid phase and dissolved substances, or it can also include suspended solids. The biofilm matrix can be

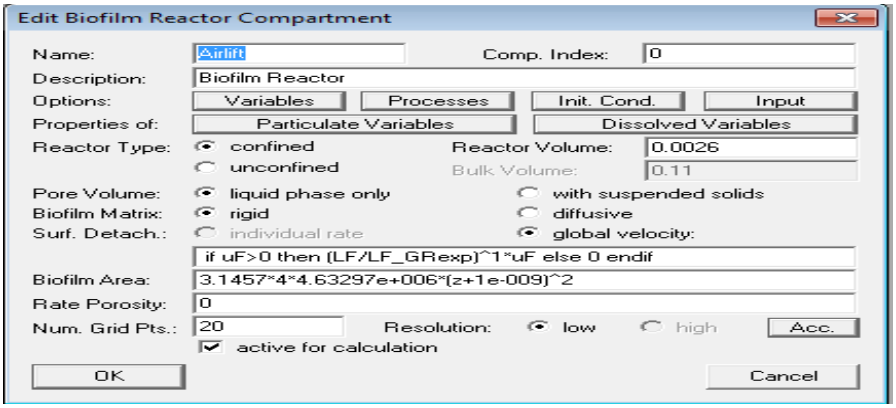

Figure 4 The AQUASIM dialog box "Edit Biofilm Reactor Compartment" is used to specify the properties of the biofilm system

predicted to be inflexible, i.e., to modify its volume due to microbial growth and decay only, or it can be predicted to be diffusive, which denotes that microbial cells can move within the

biofilm matrix also by diffusion. Separation at the biofilm surface can be explained by rates, which are properties of single microbial species and are particular thru the button "Particulate Variables." Else, it can be expressed by a global velocity, which represents that all species are detached at the same rate. The biofilm area is a uniform for a flat biofilm and is a function of the distance from the substratum for spherical or cylindrical biofilm geometry. The porosity, i.e., the fraction of the pore water volume of the biofilm, is commonly predicted to be constant. If it differs with time or space, this variation can be modelled by a rate of porosity.

The selection "Variables" acts to stimulate or deactivate variables, which signify concentrations of substrates and microbial species. For every activated variable, AQUASIM automatically computes mass balance equations for the substrates coupled with microbial species in both the biofilm and the bulk fluid. The selection "Processes" acts to stimulate or deactivate processes. Only stimulated processes are involved in the computations, whereas the value of the rates of deactivated processes is set to zero. This attribute makes it achievable to simply modify a model and to freely test alternative models. In AQUASIM, the word "Processes" means the biotic or abiotic conversion reactions. These have to be detailed by the manipulator, while the equations explaining transport processes are fundamental parts of AQUASIM. In Figure 2, it is demonstrated how the user can apply conversion reactions in AQUASIM. The model displays the rate law and the stoichiometric coefficients of the process 'heterotrophic growth." The selections "Initial Conditions" and "Input" in Figure 1 assist to support initial and influent values for the microbial species and substrates, plus for the water flow rate.

The properties of the microbial species counted are identified thru the button "Particulate Variables." Figure 3 illustrates the dialog box in which these properties can be chosen. The density, described as cell mass per unit cell volume, is the only property that must be specified at all times. AQUASIM is establishing such that extra features of the model are excluded if their parameters have a value of zero. These features comprise attachment of cells to the biofilm surface and to the solid matrix within the biofilm, single detachment of cells from the biofilm surface or solid matrix, and cell diffusion in the pore

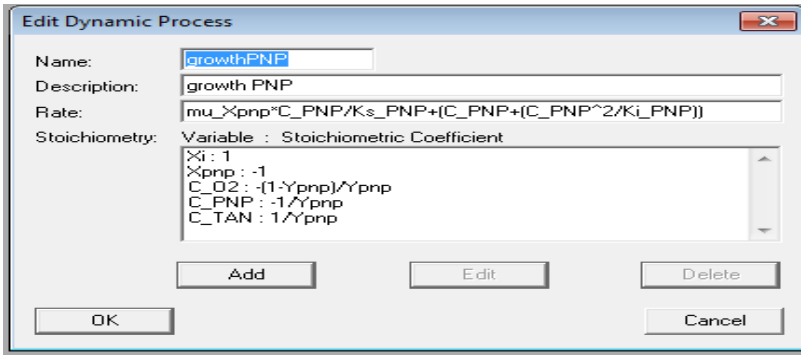

Figure 5 The AQUASIM dialog box "Edit Dynamic Process" is used to specify the rate laws and stoichiometric coefficients of biotic and abiotic conversion process

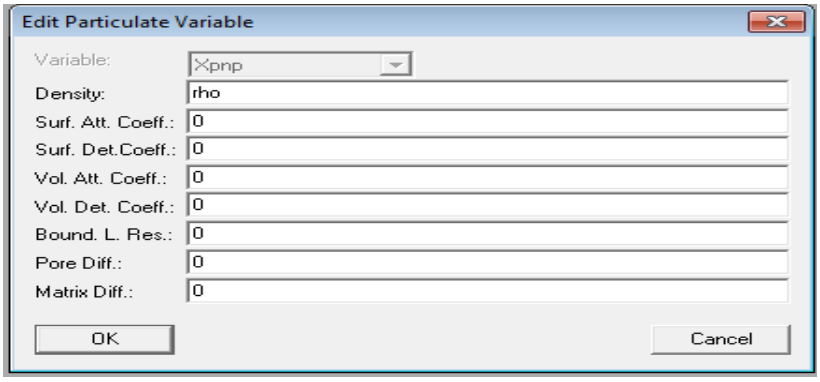

Figure 6 The AQUASIM dialog box "Edit Particulate Variable" is used to specify the properties of microbial species

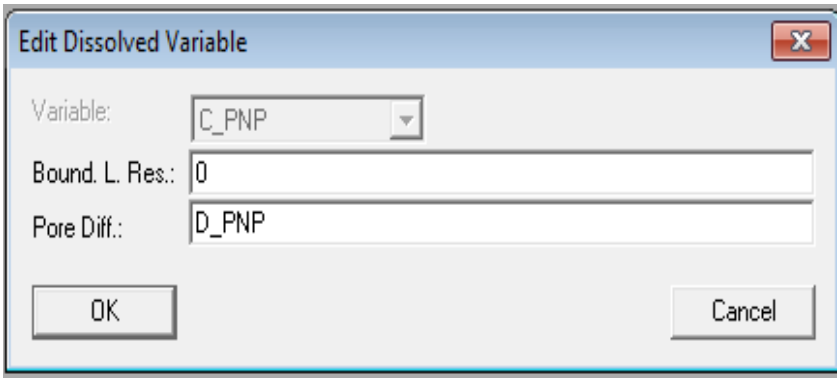

Figure 7 The AQUASIM dialog box "Edit Dissolved Variable" is used to specify the properties of dissolved substrate

water and in the solid matrix. In addition, the application of the model counts a liquid boundary layer at the biofilm surface that is neglected if the value of its resistance is set to zero. The button “Dissolved Variables” guides to a dialog box in which the properties of the dissolved substrates can be detailed (Figure 4). The diffusivity of the substrate in the pore water of the biofilm should be specified, while the boundary layer resistance can be set to

zero. In this research, the properties that will fulfil the 'Variable' are expressed in the Table 1-2 in Chapter 4.

2.5.2 Application of the model

2.5.2.1 Substrate removal

AQUASIM can be operated to model substrate elimination in a biofilm reactor. Based on the kinetics of Benchmark 3 (BM3) (Rittmann et al., 2004), the reactor substrate discharge can be analysed as a function of the substrate inflow and the growth of the biofilm in the reactor. The example in Figure 5 illustrates the substrate discharge reducing during the first days because of biofilm growth. After that, after about three days, biofilm growth and biomass detachment achieve the steady state, and the substrate discharge remains constant. Figure 5 is an original plot as it is generated by AQUASIM.

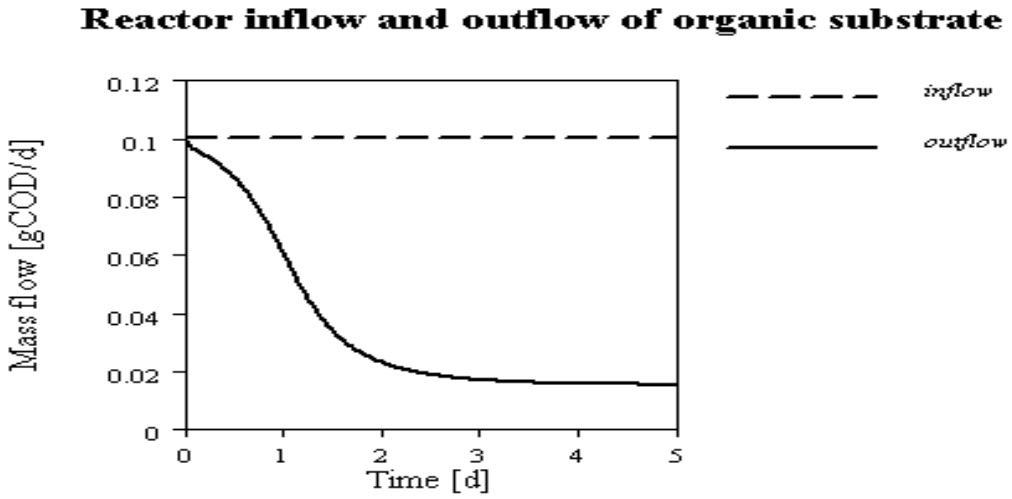

Figure 8 Typical Aquasim plot showing the development in time of the reactor inflow and outflow of organic substrate

2.5.2.2 Biofilm growth, microbial composition and detachment

AQUASIM can model biofilm growth as a result of the production of microbial mass in the biofilm. In Figure 6, a sample of the development of the thickness and microbial composition of the biofilm is presented. This example is created by the kinetics expression of Haldane-type kinetic model (Reichert,. 1998).

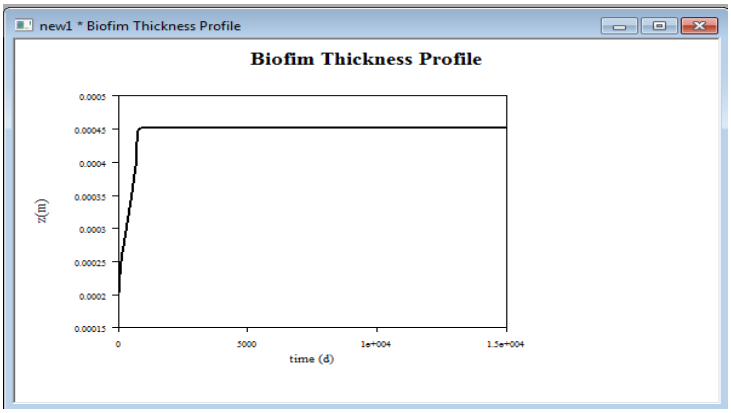

Figure 9 Development of the biofilm thickness as a function of time

In AQUASIM, a sloughing event can be modeled as

$$ude = 0.5*uF \text{ for } t \leq 19.5 \text{ days}$$

$$ude = 500*uF \text{ for } 19.51 \leq t \leq 19.52 \text{ days}$$

$$ude = 0.5*uF \text{ for } t \geq 19.53 \text{ days}$$

where ude is the global velocity of surface detachment (Figure 9) and uF is the velocity by which the biofilm surface is displaced as a result of the production and decay of microbial mass in the biofilm. Mainly, the detachment velocity ude is lesser than the production velocity uF, and the biofilm is developing. Conversely, between 19.51 and 19.52 days, ude has a value much larger than uF, leading to an increased detachment of biomass to the bulk fluid and a rapid lessen of the biofilm thickness. Between 19.5 and 19.51 days and again between 19.52 and 19.53 days, the value of ude is linearly interpolated. There are many other possibilities to model sloughing in AQUASIM, one of them is to define a base thickness above which all biofilm is detached throughout a sloughing event (Morgenroth and Wilderer, 2000; Horn et al., 2003).

2.5.2.3Limitation of the model

Like any model, the one-dimensional multi-substrate and multispecies model is based on simplifying predictions. A list of this prediction can be discovered in a recently published review on biofilm modelling. Indeed, the most significant restriction is the expectation that the biofilm is one-dimensional in space. This is obviously opposing to experimental observations, which demonstrate that a few biofilms consist of three-dimensional, mushroom

like structures. In the one-dimensional model the concentrations of substrates and microbial species are be around over planes parallel to the substratum and spatial gradients are judged in the way perpendicular to the substratum only. The standard tests have discovered that for practical intentions this is not a severe restriction; for the main microbial constituents of the biofilm solid matrix the one-dimensional model still bring in precise outcomes. Merely for the spatial distribution of specialists, i.e., of microbial species with tiny cell numbers in the biofilm could be the one-dimensional model yield results that are inaccurate.

2.5.2.4 Mathematical treatment

The mass balance equations, boundary conditions, and additional expressions required for simulations with the one-dimensional multi-substrate and multispecies biofilm model are readily accessible (Wanner and Reichert, 1996; Reichert and Wanner, 1997). However, biofilm simulation with this model needs the solution of the moving boundary problem formed by biofilm development and the solution of the stiff differential equation system of the mass balances for substrates and microbial species. In this study the mathematical model used are kinetic rate expression and they are illustrates in Table 3-4 in Chapter 4.

2.5.2.5Advantages of simulation

The advantages of simulators are that they are skilled to offer manipulator with applied respond when planning real world systems. This allows the designer to realize the exact and effectiveness of a model before the system is really constructed. By experimented the effect of particular project determinations throughout the design phase instead of the construction phase, the overall cost of building the system reduces significantly. Additional profit of simulators is that they permit system designers to investigate a problem at some different levels of concept. By approaching a system at an advanced level of constructing, the designer is better able to comprehend the activities and interactions of all the high level components within the system and is thus better provided to counteract the complexity of the overall system. This complexity may simply crush the designer if the problem had been approached from a lower level. As the designer better understands the operation of the higher level components through the use of the simulator, the lower level components may then be designed and subsequently simulated for verification and performance evaluation.

3 MATERIALS AND METHODS

3.1 Overview

This project started with the AQUASIM software familiarization. This task was conducted by doing the tutorial that was provided from the supervisor. During doing this task, the related journal paper was reviewed to obtain the parameters to be selected and analysed in the model. After that, a model was developed and the model was run with the selected parameters. Next, the simulation result was compared with the journal result. The developed models were validated so that the model simulation is compatible and produce a good correlation with the experimental data before it can be used for further study. Then, the model was used to study the several scenarios related to operational variability faced by certain industry and the data obtain was analysed.

3.2 Biofilm model, kinetics and parameters

A one-dimensional biofilm model was formed to stimulate the simultaneous nitritation and p-nitrophenol removal using aerobic granular biomass in a continuous airlift reactor performance based on Wanner and Reichert (1996) and applied in the software package AQUASIM (Reichert, 1998),v.2.1d. The reactor volume was set to be fixed at 2.6L based on the experimental data from Jemaat et al, 2013.

The biomass species depicted as particulate compounds in the biofilm matrix were five: ammonia-oxidizing bacteria (AOB), nitrite-oxidizing bacteria (NOB), p-nitrophenol degrader, heterotrophic bacteria, and inert biomass. Biofilm area was designated as a function of the granule radius, to appropriately guess the biofilm geometry. Total biofilm area was expressed as a function of granule size and number of granules. A detachment rate was operated to keep a uniform biofilm thickness in steady state at a predefined value. Detachment biomass from the biofilm was judged as active keep on the same kinetics expressed for the biomass in the biofilm. Attachment of biomass onto the biofilm surface has been ignored. For the sake of easiness external mass transfer has been ignored. The porosity of the biofilm was set as 80% and kept constant throughout the simulation. Initial fraction of particulate compound were 8% AOB,8% NOB, 2% PNP and 2% heterotrophic biomass. The microbial kinetics and the stoichiometry used are detailed in Table 3 and Table 4. Growth of AOB and NOB included inhibition by free ammonia (FA) and free nitrous acid (FNA) as

proposed by Jubany et al.,2008 .While, growth of PNP was describe as recently proposed by G.Tziotzios et al, (2008) . Decay of AOB and NOB referring to Munz et al. (2011), with a single rate equation which includes two decay coefficients: a decay coefficient for aerobic and anaerobic condition, which likely will occur in the biofilm and used in the model are detailed in Table 3, and general equation of decay rate is used for decay of PNP.

Table 3: Kinetic parameter

Symbol	Definition	Value	Unit	References
Ammonium oxidizing bacteria (AOB)				
$\mu_{max,AOB}$	Maximum Specific growth rate of X_{AOB}	2.3	d^{-1}	Jubany et al. (2008)
$b_{AER,AOB}$	Decay rate	0.6	d^{-1}	Munz et al. (2011)
$b_{ANAER,AOB}$	Anaerobic decay rate	0.025	d^{-1}	Munz et al. (2011)
Y_{AOB}	Growth yield	0.18	$gCODg^{-1}N$	Jubany et al. (2008)
$K_{O2,AOB}$	Affinity constant for oxygen	0.74	mgO2/L	Guisasola et al. (2005)
$K_{S,TAN}$	Affinity constant for TAN	11	mgTAN/L	Carrera et al. (2004)
$K_{I,TAN,AOB}$	Inhibition coefficient for TAN	675	mgTAN/L	Jubany et al. (2009)
$K_{I,TNN,AOB}$	Inhibition coefficient for TNN	13115	mgTNN/L	Jubany et al. (2009)
$K_{I,PNP,AOB}$	Inhibition coefficient for PNP	7	$gPNP/m^3$	Jemaat et al.(2013a)
Nitrite-oxidizing bacteria (NOB)				
$\mu_{max,NOB}$	Maximum Specific growth rate of X_{NOB}	1.65	d^{-1}	Jubany et al. (2008)
$b_{AER,NOB}$	Decay rate	0.25	d^{-1}	Munz et al. (2011)
$b_{ANAER,NOB}$	Anaerobic decay rate	0.012	d^{-1}	Munz et al. (2011)
Y_{NOB}	Growth yield	0.08	$gCODg^{-1}N$	Jubany et al. (2008)
$K_{O2,NOB}$	Affinity constant for oxygen	1.75	mgO2/L	Guisasola et al. (2005)
$K_{S,TNN}$	Affinity constant for TNN	22	mgTNN/L	Ni et al. (2008)
$K_{I,TAN,NOB}$	Inhibition coefficient for TAN	145	mgTAN/L	Jubany et al. (2008)
$K_{I,TNN,NOB}$	Inhibition coefficient for TNN	1431	mgTNN/L	Brockman and Morgenroth (2010)
***P*-nitrophenol degradation**				
$\mu_{max,PNP}$	Maximum Specific growth rate of X_{PNP}	0.406	d^{-1}	Martín-Hernández et al. (2009)
b_{PNP}	Decay rate	0.212	d^{-1}	Tomei et al.(2004)

Y_{PNP}	Growth yield	0.28	$gCODg^{-1}N$	Martín-Hernández et al. (2009
$K_{O2,PNP}$	Affinity constant for oxygen	1.65	mgO2/L	Jemaat et al. (2013a)
$K_{S,PNP}$	Affinity constant for PNP	1.6	mgPNP/L	Martín-Hernández et al. (2009
$K_{I,PNP}$	Inhibition coefficient for PNP	54	mgPNP /L	Martín-Hernández et al. (2009
Heterotrophic bacteria (H)				
μ_H	Maximum Specific growth rate of X_H	11.8	d^{-1}	Henze et al. (2000)
b_H	Decay rate	7.87	d^{-1}	Henze et al. (2000)
Y_H	Growth yield	0.67	$gCODg^{-1}N$	Henze et al. (2000)
$K_{O2,H}$	Affinity constant for oxygen	0.2	mgO_2/L	Henze et al. (2000)
$K_{S,S}$	Affinity constant for substrate	4	mgCOD/L	Henze et al. (2000)

Table 4: Diffusivity

Parameter	Symbol	Value	Unit	References
Diffusivity of O_2 in water	D_{O2}	2.2×10^{-4}	m^2d^{-1}	Picioreanu et al.(1997)
Diffusivity of NH4+ in water	D_{TAN}	1.9×10^{-4}	m^2d^{-1}	Picioreanu et al.(1997)
Diffusivity of NO2- in water	D_{TNN}	1.7×10^{-4}	m^2d^{-1}	Picioreanu et al.(1997)
Diffusivity of NO3- in water	D_{NO3}	1.7×10^{-4}	m^2d^{-1}	Picioreanu et al.(1997)
Diffusivity of PNP in water	D_{PNP}	1.7×10^{-4}	m^2d^{-1}	Spigno et al.(2004)
Diffusivity of organic substrate in water	D_S	1.0×10^{-4}	m^2d^{-1}	Picioreanu et al.(1997)
Diffusivity coefficient inside biofilm	E_{Diff}	0.5	Dimensionless	Assumed in the range proposed by Bishop et al.(1995)

Table 5: Kinetic expression

j	Process	Process rate (d^{-1})	References
1	Growth of X_{AOB}	$\mu_{max\_AOB} \cdot \frac{SO2}{KO2,AOB+SO2} \cdot \frac{STAN}{KS,TAN,AOB+STAN+\frac{STAN^2}{KI,TAN,AOB}} \cdot \frac{KI,TAN,AOB}{KI,TAN,AOB+STNN} \cdot \frac{KI,PNP,AOB}{KI,PNP,AOB+SPNP} \cdot X_{AOB}$	Jubany et al.(2008)
	Decay of X_{AOB}	$b_{AER,AOB} \cdot \frac{SO2}{KO2,AOB+S02} \cdot X_{AOB} + b_{ANAER,AOB} \cdot X_{AOB}$	Munz et al.(2011)
2	Growth of X_{NOB}	$\mu_{max\_NOB} \cdot \frac{SO2}{KO2,NOB+SO2} \cdot \frac{STNN}{KS,TNN,NOB+STNN+\frac{STNN^2}{KI,TNN,AOB}} \cdot \frac{KI,TAN,NOB}{KI,TAN,NOB+STNN} \cdot X_{NOB}$	Jubany et al.(2008)
	Decay of X_{NOB}	$b_{AER,NOB} \cdot \frac{SO2}{KO2,NOB+S02} \cdot X_{NOB} + b_{ANAER,NOB} \cdot X_{NOB}$	Munz et al.(2011)
3	Growth of X_H	$\mu_{max\_H} \cdot \frac{SO2}{KO2,H+SO2} \cdot \frac{SS}{KS,H+SS} \cdot X_H$	Henze et al.(2000)
	Decay of X_H	$b_H \cdot X_H$	Henze et al.(2000)
4	Growth of X_{PNP}	$\mu_{max,PNP} \cdot \frac{S_{PNP}}{K_{S,PNP}+S,PNP+\frac{S_{PNP}^2}{K_{I,PNP}}}$	Tziotzios et al, (2008)
	Decay of X_{PNP}	$b_{PNP} \cdot X_{PNP}$	General equation for decay rate

Table 6 :Stoichiometric Matrix

j	Process	S_{O2}	S_{TAN}	S_{TNN}	S_{NO3}	S_S	S_{PNP}	X_{AOB}	X_{NOB}	X_H	X_I	X_{PNP}
1	Growth of X_{AOB}	$-(3.43 - Y_{AOB}) / Y_{AOB}$	-1 / YAOB	$1/Y_{AOB}$				1				
2	Decay of X_{AOB}							-1			1	
3	Growth of X_{NOB}	$-(1.14 - Y_{NOB}) / Y_{NOB}$		$-1 / Y_{NOB}$	$1 / Y_{NOB}$				1			
4	Decay of X_{NOB}								-1		1	
5	Growth of X_{PNP}	$-(1-Y_{PNP})/Y_{PNP}$		$1 / Y_{PNP}$			$-1 / Y_{PNP}$				1	-1
6	Decay of X_{PNP}										1	-1
7	Growth of X_H	$-(1 - Y_H) / Y_H$				$-1 / Y_H$						
8	Decay of X_H											
	Units	gO_2m^{-3}	gNm^{-3}	gNm^{-3}	gNm^{-3}	$gCOD\ m^{-3}$	$gCOD\ m^{-3}$	$gCOD\ m^{-3}$	$gCOD\ m^{-3}$	$gCOD\ m^{-3}$	$gCOD\ m^{-3}$	$gCOD\ m^{-3}$

3.3Modelling the TAN control loop inside the ratio control strategy

Modelling the TAN control loop inside the ratio control strategy proposed by Jemaat et al,.(2013b) titled closed-loop control of ammonia concentration in nitritation is practically used in this research. The control strategy has two dissimilar closed-loops: (i) one to uphold the AOB concentration in the bulk liquid (i.e., the reactor effluent, considering a well-mixed liquid phase in the reactor) and (ii) a second one to control the DO concentration in the bulk liquid. Each one of these two control loops has to be connected within the proportionality constant (R_{SP} to become a true ratio control strategy (Jemaat et al, 2013b).

For the mathematical explanation of the DO control loop, aeration was presented as a dynamic process only practising in the bulk liquid phase. A high value for the volumetric gas-liquid oxygen transfer coefficient ($k_{La} = 10^4 d^{-1}$) was selected. The oxygen solubility used was alike to the DO set point (Jemaat et al,2013b).

$$\frac{d[DO]}{dt} = k_L a^{sup}.([DO*] - [DO]) - (OUR_{end} + OUR_{max}).\frac{[DO]}{[DO] + K_O^{PNP}} \quad (1)$$

Where $k_L a^{sup}$ is the global oxygen mass transfer constant through the liquid surface (d^{-1}), [DO*] is the DO concentration at saturation ($mgO_2L^{-1}d^{-1}$), [DO] is the DO concentration ($mgO_2L^{-1}d^{-1}$), OUR end is the endogenous OUR value ($mgO_2L^{-1}d^{-1}$), OUR max is the maximum OUR value ($mgO_2L^{-1}d^{-1}$) and K_O^{PNP} is the oxygen half-saturation coefficient for PNP-degraders (mgO_2L^{-1}).

For the TAN control loop, an ad hoc expression was developed, because the control loop has the inflow rate Qin as manipulated variable:

$$Q_{in} = Q_{in,0}.\left(1 + \frac{[TAN]_{SP} - [TAN]}{[TAN]_{SP}}.a\right) \quad (2)$$

Where $Q_{in,0}$ is identified as the preference of the control action, i.e. the default value of flow-rate. The controller will always act either rising or $reducing\ Q_{in}$ around$Q_{in,0}$. [TAN] is the concentration in the bulk liquid phase. $[TAN]_{SP}$ is the TAN concentration set point. a is the proportional gain of the controller, easily tuned in each simulation depending on the particular operating conditions. The principle of the performance of the expression is similar to that applied in a conventional proportional control law. The action will be stronger when the measured value of TAN concentration is far from the set point, whereas when TAN concentration is approaching the set point, the action of the controller will be weaker (Jemaat et al., 2013b)

The set points were linked through the proportionality constant (R_{SP}) as

$$[DO_{SP}] = R_{SP}.[TAN]_{SP} \quad (3)$$

3.4Simulation strategy for model validation

The steady states experimentally achieved by (Jemaat et al., 2013a) were counted for the justification of the mathematical model as shown in appendix (Table A4 and Table A5). Working conditions and several key investigational measurements were used as feeds for the model in each one of the stable conditions counted. Particularly, experimental data of $V_{reactor}$ is directly used for the determination of nitrogen loading rate (NLR) and PNP loading rate (PNP-LR) as shown in the equation 4 and equation 5 below:

$$NLR = \frac{Qtot \times [TAN]in}{V_{reactor}} \quad (4)$$

$$PNP - LR = \frac{Qtot \times [PNP]in}{V_{reactor}} \quad (5)$$

Where

[TAN] = Initial concentration for TAN

[PNP] = Initial concentration for PNP

Q_{tot} = Total flowrate

Consequently, the total flowrate (Q_{tot}) is presented in AQUASIM via the expression:

$$Q_{tot} = Q_{QVar} + Q_{in} \quad (6)$$

Where Q_{Qvar} stands for the variation for the flow rate in the biofilm until achieve steady state value (declared as a formula variable in AQUASIM). Steady state flow rate was imposed to be equal to the experimental one. To assure steady state in the simulations, they were run for a period of operation of 15000 days, and results in terms of concentrations in the bulk liquid were inspected to check that constant values were achieved.

4 RESULT AND DISCUSSION

4.1 Model validation

For model validation a set of experimental results in steady state previously published in Jemaat et al., (2013a) were considered and they were detailed in appendix (Table A1 and Table A2). The model was able to predict when full simultaneous nitritation and p-nitrophenol removal is maintained at steady state for experimental periods at 30°C (Table5, for a direct comparison of model comparison and experimental result). Note how the modelling result show a good agreement with experimental result when the Nitrogen Loading rate (NLR) and PNP Loading rate give a good correlation. Experimentally, the maximum value of NLR that could lead to simultaneous nitritation and PNP removal in steady state were narrowed within 1.1 gNL-1d-1 and 15.9 mg PNP L-1 d-1 ,respectively (Jemaat et al.,2013a), and this is same range found through simulation and presented in appendix (Figure A1 to Figure A3).

Another output of the model was the concentration for TAN, Total Nitrite Nitrogen (TNN), NO3 and PNP in the effluent. Direct comparison of the experimental concentration with that obtained in the simulations is also presented in Table 1. The mathematical model was able to predict the trend although there were some deviations.

Table 7 Model validation. Comparison of experimental result obtained in steady state and simulation result.

pH	Temperature	Nitrogen Loading rate (NLR)		PNP-Loading rate (PNP-LR)		TAN converted to TNN %		TAN converted to Nitrite %		PNP-degraded %	
		Exp.	Model	Exp.	Model	Exp.	Model	Exp.	Model	Exp.	Model
8.2	30 °C	1.1	1.3	15.9	17.3	85	98	0.3	0	95	92.3

4.2 Effect of the TAN and PNP effluent concentration on the applied loading rate.

Experimental conditions in Table 1 were used to explore how the TAN and PNP effluent concentration affects the applied volumetric nitrogen loading rate (NLR_v) and PNP loading rate for a wide range of values. The results obtained with this set of simulations are presented in Figure 10 and Figure 11. The specific set points considered in the simulation presented in Figure 10 and Figure 2 is detailed in appendices (Table 1 and Table 2).

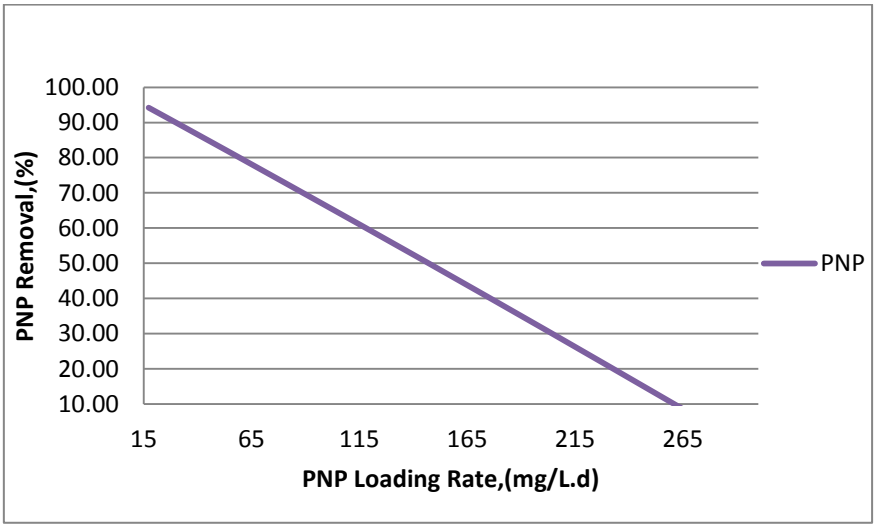

Figure 10 Graph of percentage PNP removal versus PNP loading rate

Figure 10 above illustrates the effect of PNP loading rate to the PNP removal. From figure 10, it shows that when PNP loading rate increase, the percentage removal of the PNP in the reactor effluent is decreased. This signifies that, increasing the PNP loading will decrease the PNP removal efficiency. The highest PNP removal can be achieved at 17.31 mg/L.d with the percentage removal is 94.2 %. While, the lowest PNP removal is at 288.5 mg/L.d of PNP loading rate which is 0.27 %.

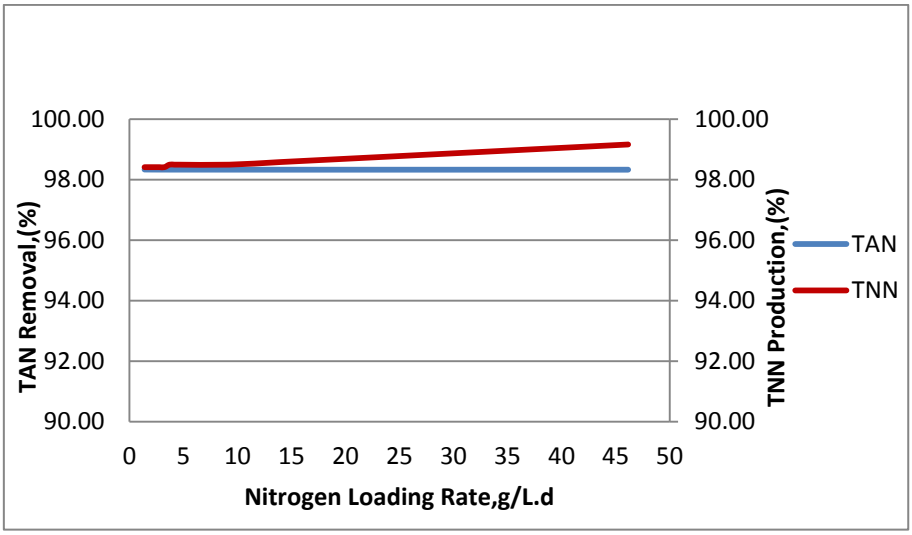

Figure 11 Graph of TAN removal and TNN production versus Nitrogen Loading rate

Figure 11 above shows the graph of percentage removal of TAN and TNN production versus nitrogen loading rate (NLR). From the graph, for TAN curve, it shows that percentage removal of TAN is always maintained above 98% throughout the simulation even though there are increased in NLR. This result indicate the efficiency of the system to maintain the percentage removal for TAN since the used of control system is applied. Thus, it can be conclude that increasing the NLR to the maximum value will not influence the TAN removal if the control system is applied. While, for TNN curve, it demonstrates that in the beginning, increasing NLR from 1.34 $gL^{-1}d^{-1}$ to 13.85 $gL^{-1}d^{-1}$, there is a constant percentage for TNN production. But, continuously increase the NLR to the maximum value also increase the TNN production for the system. The maximum value for NLR is 46.15 $gL^{-1}d^{-1}$ and the maximum percentage TNN production is 99.17%.

4.3 Effect of temperature

Temperature has a significant effect on the reaction kinetics. The rate constant for PNP,AOB,NOB,heterotropic bacteria and inert biomass is in the function of temperature was included in the simulation as shown in appendix (Table A3).

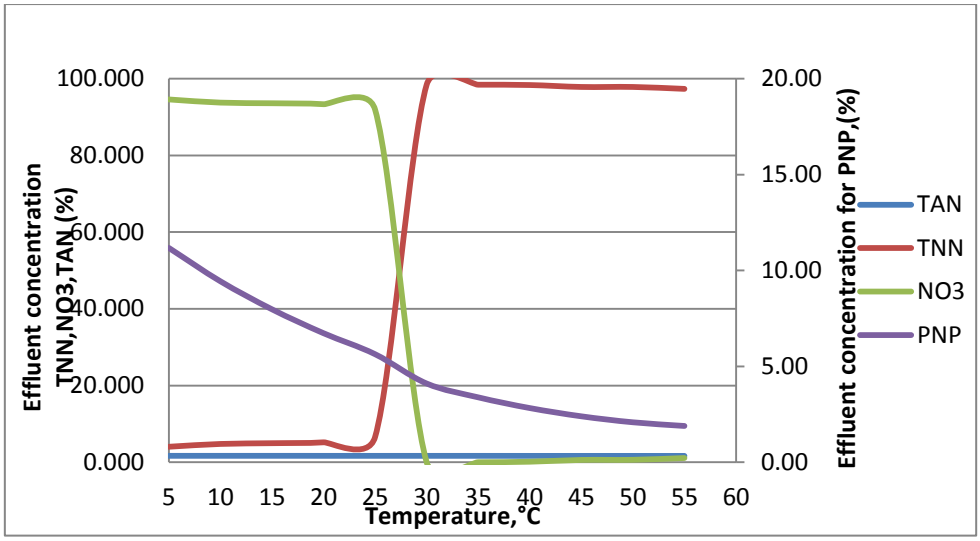

Figure 12 Graph of percentage effluent concentration versus temperature

Figure 12 above designate the association for temperature and the percentage of effluent concentration. From the Figure 12 above, we noticed that the higher temperature condition for this system is 55°C and the minimum temperature is 5 °C.The graph shows, the minimum temperature has occur nitrification reaction since the production of nitrate is highest. It is commonly known that nitrification rate is significantly decreased at low temperature. But, nitrification rate remain high when temperature dropped from 25°C to 5°C as shown in Figure 3. It seemed the autotrophic biofilm in airlift reactor could alleviate the temperature effect. While in temperature 26°C the simultaneous nitritation starting to predominant. The trending for the graph shows, increasing temperature, will increase the simultaneous nitritation and PNP removal. This is because, when the temperature of the rate constant is increased, the value of rate constant is also increase respectively. The increase in rate constant with higher temperature is due to the easier cavitation as a result of higher vapour pressure of solution (Mason,1999). Increase in temperature increase the number of cavitation bubbles and hence hydroxyl radicals and nitro radicals consequently an increased degradation rates.

In the temperature approximately at 27°C, from the figure 3 above, it shows that the percentage of effluent concentration for TAN and TNN is 50 %. Thus, in this condition, the anaerobic denitrification process can be further for ammonia removal.

4.4 Effect of pH

In water and wastewater treatment, pH is a crucial parameter. The effects of pH change for the simultaneous nitritation and PNP removal were investigated by varying the pH under constant process parameter. Figure 13 shows the results of the effects of pH on the simultaneous nitritation and PNP removal.

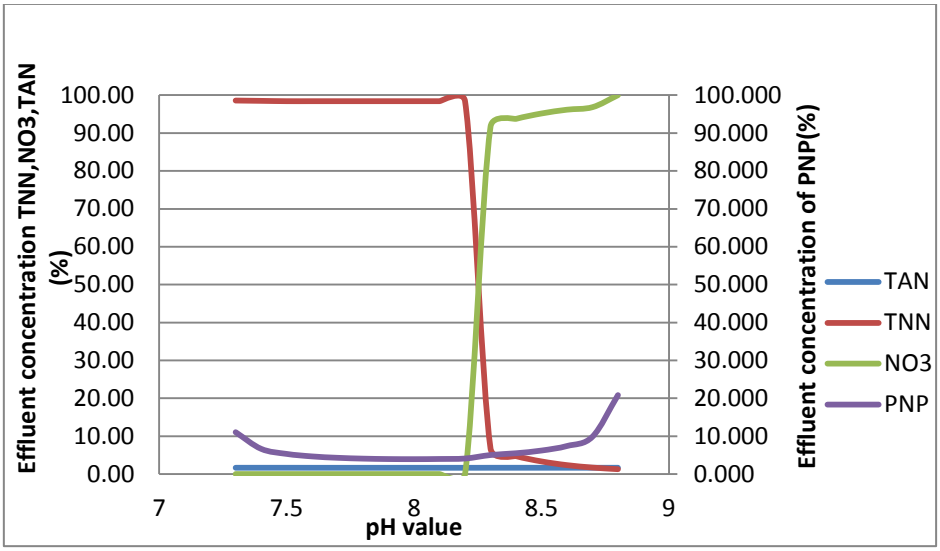

Figure 13 Graph of percentage effluent concentration versus pH value

From the results in Figure 13, it can be observed that the simultaneous nitritation and PNP removal only happen in pH range between 7.3 and 8.2. While, at pH range from 8.3 to 8.8, the nitrification process is take place for ammonia removal since the TAN is almost converted to nitrate. The trending removal for PNP is increase at pH 7.3 to 8.2 and then starting to decrease at pH 8.3 to 8.8. Because of the used control-loop for TAN, the effluent concentration for TAN is always constant throughout the simulation. The difference in degradation rate for PNP between the pH 7.3 to 7.7 is relatively low consistent with the finding of Carrera et al.,(2011) in the modelling the pH dependence of the kinetics of aerobic p-nitrophenol biodegradation. However, at pH between 8.3 and 8.8, it is observed that the degradation of PNP was significantly increase. This is consistence with the reports of pH having significant effect in certain organics at alkaline pH ranges (Mendez-Arriage et al., 2008; Torres et al., 2008).

4.5 Effect of effluent concentration on the applied initial value concentration of PNP

The effect of initial PNP concentration was investigated, and the simulation experiment was carried out from 20 g/m^3 up to 1000g/m^3 of individual PNP concentration. It can be seen in Figure 14 that the percentage removal efficiency with time relative to the initial concentration is inversely related to the initial concentration of the PNP.

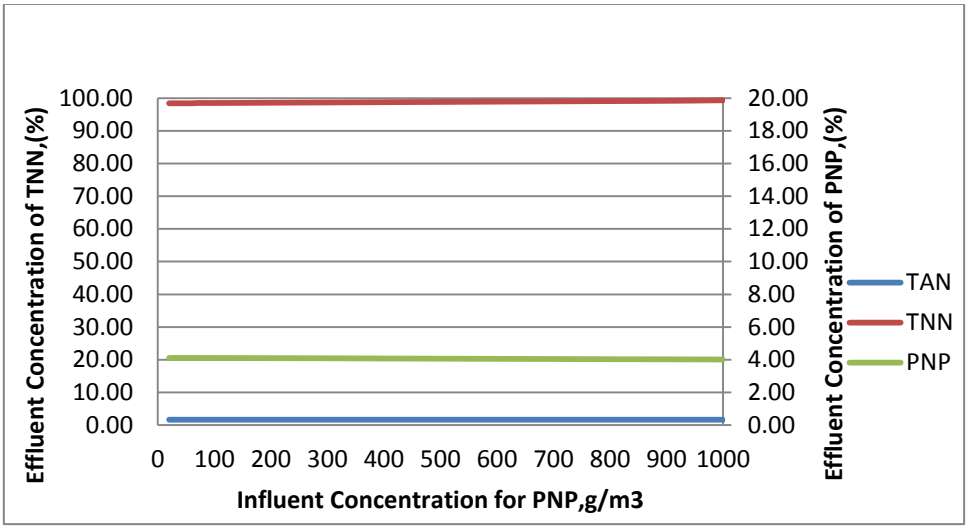

Figure 14 Graph of percentage Effluent Concentration versus Influent Concentration of PNP

Figure 14 above specify the relationship of the influent concentration of PNP in the airlift reactor and the concentration for the reactor effluent in simultaneous nitritation and PNP removal. From figure 14, it shows that the highest percentage concentration in the reactor effluent is TNN with 99.17% followed by 4.01% of PNP and 1.66% of TAN. This result is almost similar to the experimental result obtained previously with 15mg/l of initial PNP concentration. The constant percentage concentrations of TAN in the effluent showed that, the control system used in this study have a good performance in controlling the system variable so that the set point can be achieved. In addition, it proved that the granular biomass is batter able to cushion the effect of an inhibitory compound since there is no TAN accumulation that might expected when PNP concentration is more than 7 mg/l. Thus, the results indicate that the simultaneous nitritation and PNP removal system almost was not affected by the initial PNP concentration.

5 CONCLUSION

This paper discusses the feasibility for modelling simultaneous nitrification and biological removal of phenol in an activated sludge could be successfully applied in AUASIM biofilm reactor compartment. The system was able to degrade initial phenol concentrations up to 1000 g/m^3. Results of this tests show that the optimum pH was around 7.3 to 8.3, whereas the temperature showed no significant impact on phenol biodegradation rates over the investigated conditions but for ammonia, the maximum temperature for nitrification process is at 55°C. Specific simultaneous nitrification and phenol biodegradation rates in the sludge followed the Haldane model because of substrate inhibition, and reached maximum at 400 mgL^{-1} VSS at the phenol concentration of 15 g/m^3 at pH 8.2 and 30 °C, based on experimental result. From the simulated result it showed that the maximum capacity of the reactor to treat simultaneous nitritation and PNP removal were 46.15 gN $L^{-1}d^{-1}$ and 288.5 mg PNP $L^{-1}d^{-1}$. Therefore, this study demonstrated the feasibility of modelling simultaneous nitrification and biological removal of phenol in an activated sludge for the effective simultaneous nitrification and biodegradation of phenols in varies parameter condition desired.

6 REFERENCES

Adav, S. S., Lee, D.-J., & Lai, J.-Y. (2009). Treating chemical industries influent using aerobic granular sludge: Recent development. *Journal of the Taiwan Institute of Chemical Engineers, 40*(3), 333-336. doi: 10.1016/j.jtice.2009.02.002

Adav, S. S., Lee, D.-J., Show, K.-Y., & Tay, J.-H. (2008). Aerobic granular sludge: Recent advances. *Biotechnology Advances, 26*(5), 411-423. doi: 10.1016/j.biotechadv.2008.05.002

Béline, F., Boursier, H., Daumer, M. L., Guiziou, F., & Paul, E. (2007). Modelling of biological processes during aerobic treatment of piggery wastewater aiming at process optimisation. *Bioresource Technology, 98*(17), 3298-3308. doi: 10.1016/j.biortech.2006.07.004

Carrera, J., Martín-Hernández, M., Suárez-Ojeda, M. E., & Pérez, J. (2011). Modelling the pH dependence of the kinetics of aerobic p-nitrophenol biodegradation. *Journal of Hazardous Materials, 186*(2-3), 1947-1953. doi: 10.1016/j.jhazmat.2010.12.096

Choquette-Labbé, M., Shewa, W., Lalman, J., & Shanmugam, S. (2014). Photocatalytic Degradation of Phenol and Phenol Derivatives Using a Nano-TiO2 Catalyst: Integrating Quantitative and Qualitative Factors Using Response Surface Methodology. *Water, 6*(6), 1785-1806. doi: 10.3390/w6061785

Faulwetter, J. L., Gagnon, V., Sundberg, C., Chazarenc, F., Burr, M. D., Brisson, J., . . . Stein, O. R. (2009). Microbial processes influencing performance of treatment wetlands: A review. *Ecological Engineering, 35*(6), 987-1004. doi: 10.1016/j.ecoleng.2008.12.030

Ganigué, R., Volcke, E. I. P., Puig, S., Balaguer, M. D., & Colprim, J. (2012). Impact of influent characteristics on a partial nitritation SBR treating high nitrogen loaded wastewater. *Bioresource Technology, 111*, 62-69. doi: 10.1016/j.biortech.2012.01.183

Ifelebuegu, A. O., Onubogu, J., Joyce, E., & Mason, T. (2013). Sonochemical degradation of endocrine disrupting chemicals 17β-estradiol and 17α-ethinylestradiol in water and wastewater. *International Journal of Environmental Science and Technology, 11*(1), 1-8. doi: 10.1007/s13762-013-0365-2

Jemaat, Z., Bartrolí, A., Isanta, E., Carrera, J., Suárez-Ojeda, M. E., & Pérez, J. (2013b). Closed-loop control of ammonium concentration in nitritation: Convenient for reactor operation but also for modeling. *Bioresource Technology, 128*, 655-663. doi: 10.1016/j.biortech.2012.10.045

Jemaat, Z., Suárez-Ojeda, M. E., Pérez, J., & Carrera, J. (2013a). Simultaneous nitritation and p-nitrophenol removal using aerobic granular biomass in a continuous airlift reactor. *Bioresource Technology, 150,* 307-313. doi: 10.1016/j.biortech.2013.10.005

Jin, R.-C., Zheng, P., Mahmood, Q., & Zhang, L. (2008). Performance of a nitrifying airlift reactor using granular sludge. *Separation and Purification Technology, 63*(3), 670-675. doi: 10.1016/j.seppur.2008.07.012

Jubany, I., Carrera, J., Lafuente, J., & Baeza, J. A. (2008). Start-up of a nitrification system with automatic control to treat highly concentrated ammonium wastewater: Experimental results and modeling. *Chemical Engineering Journal, 144*(3), 407-419. doi: 10.1016/j.cej.2008.02.010

Jubany, I., Lafuente, J., Baeza, J. A., & Carrera, J. (2009). Total and stable washout of nitrite oxidizing bacteria from a nitrifying continuous activated sludge system using automatic control based on Oxygen Uptake Rate measurements. *Water Research, 43*(11), 2761-2772. doi: 10.1016/j.watres.2009.03.022

Kiran Kumar Reddy, G., Nancharaiah, Y. V., & Venugopalan, V. P. (2014). Biodegradation of dibutyl phosphite by Sphingobium sp. AMGD5 isolated from aerobic granular biomass. *International Biodeterioration & Biodegradation, 91*, 60-65. doi: 10.1016/j.ibiod.2014.03.010

Lee, D.-J., Chen, Y.-Y., Show, K.-Y., Whiteley, C. G., & Tay, J.-H. (2010). Advances in aerobic granule formation and granule stability in the course of storage and reactor operation. *Biotechnology Advances, 28*(6), 919-934. doi: 10.1016/j.biotechadv.2010.08.007

Marrot, B., Barrios-Martinez, A., Moulin, P., & Roche, N. (2006). Biodegradation of high phenol concentration by activated sludge in an immersed membrane bioreactor. *Biochemical Engineering Journal, 30*(2), 174-183. doi: 10.1016/j.bej.2006.03.006

Mascolo, G., Balest, L., Cassano, D., Laera, G., Lopez, A., Pollice, A., & Salerno, C. (2010). Biodegradability of pharmaceutical industrial wastewater and formation of recalcitrant organic compounds during aerobic biological treatment. *Bioresource Technology, 101*(8), 2585-2591. doi: 10.1016/j.biortech.2009.10.057

Maszenan, A. M., Liu, Y., & Ng, W. J. (2011). Bioremediation of wastewaters with recalcitrant organic compounds and metals by aerobic granules. *Biotechnology Advances, 29*(1), 111-123. doi: 10.1016/j.biotechadv.2010.09.004

Mburu, N., Rousseau, D. P. L., Stein, O. R., & Lens, P. N. L. (2014). Simulation of batch-operated experimental wetland mesocosms in AQUASIM biofilm reactor

compartment. *Journal of Environmental Management, 134*, 100-108. doi: 10.1016/j.jenvman.2014.01.005

Méndez-Arriaga, F., Esplugas, S., & Giménez, J. (2008). Photocatalytic degradation of non-steroidal anti-inflammatory drugs with TiO2 and simulated solar irradiation. *Water Research, 42*(3), 585-594. doi: 10.1016/j.watres.2007.08.002

Munz, G., Lubello, C., & Oleszkiewicz, J. A. (2011). Modeling the decay of ammonium oxidizing bacteria. *Water Research, 45*(2), 557-564. doi: 10.1016/j.watres.2010.09.022

Rezouga, F., Hamdi, M., & Sperandio, M. (2009). Variability of kinetic parameters due to biomass acclimation: Case of para-nitrophenol biodegradation. *Bioresource Technology, 100*(21), 5021-5029. doi: 10.1016/j.biortech.2009.05.039

Salehi, Z., Sohrabi, M., Vahabzadeh, F., Fatemi, S., & Kawase, Y. (2010). Modeling of p-nitrophenol biodegradation by Ralstonia eutropha via application of the substrate inhibition concept. *Journal of Hazardous Materials, 177*(1-3), 582-585. doi: 10.1016/j.jhazmat.2009.12.072

Sonnad, J. R., & Goudar, C. T. (2004). Solution of the Haldane equation for substrate inhibition enzyme kinetics using the decomposition method. *Mathematical and Computer Modelling, 40*(5-6), 573-582. doi: 10.1016/j.mcm.2003.10.051

Spigno, G., Zilli, M., & Nicolella, C. (2004). Mathematical modelling and simulation of phenol degradation in biofilters. *Biochemical Engineering Journal, 19*(3), 267-275. doi: 10.1016/j.bej.2004.02.007

Torres, R., Petrier, C., Combet, E., Carrier, M., & Pulgarin, C. (2008). Ultrasonic cavitation applied to the treatment of bisphenol A. Effect of sonochemical parameters and analysis of BPA by-products. *Ultrasonics Sonochemistry, 15*(4), 605-611. doi: 10.1016/j.ultsonch.2007.07.003

Wang, N., Zheng, T., Jiang, J., Lung, W.-s., Miao, X., & Wang, P. (2014). Pilot-scale treatment of p-Nitrophenol wastewater by microwave-enhanced Fenton oxidation process: Effects of system parameters and kinetics study. *Chemical Engineering Journal, 239*, 351-359. doi: 10.1016/j.cej.2013.11.038

Zhou, D., Liu, M., Wang, J., Dong, S., Cui, N., & Gao, L. (2013). Granulation of activated sludge in a continuous flow airlift reactor by strong drag force. *Biotechnology and Bioprocess Engineering, 18*(2), 289-299. doi: 10.1007/s12257-012-0513-4

7 APPENDICES

7.1 Biological process

Nitrification was defined as two –step process with a first oxidation of ammonia to nitrite by ammonium-oxidizing bacteria (AOB) and subsequent oxidation of nitrite to nitrate by nitrite-oxidizing bacteria (NOB).

Stochiometric and kinetic parameter values together with their corresponding rate expression are presented in Table 3, Table 4, Table 5, and Table 6. All the kinetic parameters were taken from literature. A temperature correction as applies through Eq. (A1) to the kinetic parameter corresponding to the heterotrophic biomass as proposed by Henze et al.(2000).

$$k(T) = k(20°C)e^{0.07\,(T-20°C)} \quad \text{(A1)}$$

Where k is μ_{max} or b_H and T is the temperataure (°C)

The value corresponding to the maximum specific $\mu_{max,AOB}$ and $\mu_{max,NOB}$) were calculated with the equation proposed by Jubany et. al (2008) while for $\mu_{max,PNP}$ were calculated with the equation proposed by Carera et. al (2011), growth rate of autotrophic bacteria and define in AQUASIM as follows :

$$\mu_{max,AOB}(pH,T) = 3.868 * (1.07\text{^}(T-30))/(Ks\_PNP + C\_PNPini + (C\_PNPini/ Ki\_PNP * ((1 + 10\text{^}(pH - 7.15)\text{^}2)))) \quad \text{(A2)}$$

$$\mu_{max,NOB}(pH,T) = 6.67e+007 * exp(-5295/(273+T))/(1 + ((2.05e-009)/ 10\text{^}(-pH)) + (10\text{^}(-pH)/(1.66e-007))) \quad \text{(A3)}$$

$$\mu_{max,PNP}(pH,T) = 3.868 * (1.07\text{^}(T-30))/(Ks\_PNP + C\_PNPini + (C\_PNPini/ Ki\_PNP * ((1 + 10\text{^}(pH - 7.15)\text{^}2)))) \quad \text{(A4)}$$

On the other hand, the decay rate expression for AOB and NOB were calculated with the equations proposed by Munz et al. (2011), while decay rate expression for PNP were

calculated by used the equation for heterotrophic bacteria and they are modified with the temperature correction and was defined in AQUASIM as follows:

$$b_{AER,AOB}(T) = 3.21343e+011 * exp((-8183/(273+T))) \quad \text{(A5)}$$

$$b_{ANAER,AOB}(T) = 1.339e+010 * exp((-8183/(273+T))) \quad \text{(A6)}$$

$$b_{AER,NOB}(T) = 9.71278e+006 * exp(-5295/(T+273)) \quad \text{(A7)}$$

$$b_{ANAER,NOB}(T) = 466200 * exp(-5295/(T+273)) \quad \text{(A8)}$$

$$b_{PNP}(T) = 0.212 * (1.07)\text{^}(T-30) \quad \text{(A9)}$$

The terms TAN and TNN were used instead of ammonium and nitrite in Table 3, Table 4, Table 5 and Table 6 because they are the true compound analysed in the chemical analysis.

7.2 AQUASIAM result

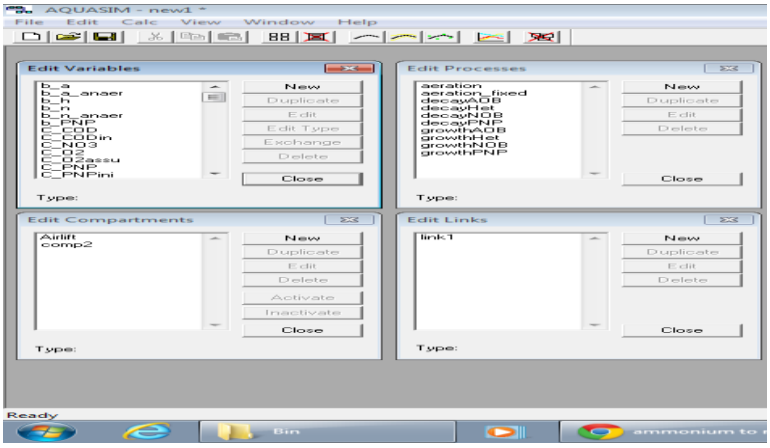

Figure 15 The AQUASIM dialog box "Edit system" to specify variable,process, compartment and link

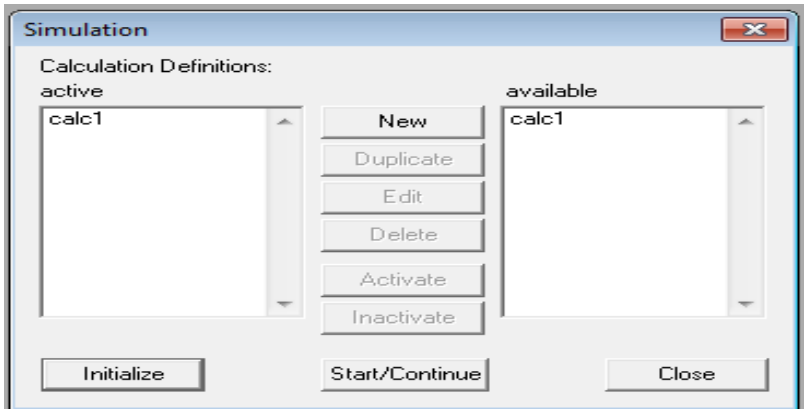

Figure 16 The AQUASIM dialog box 'Simulation' to specify calculation definition

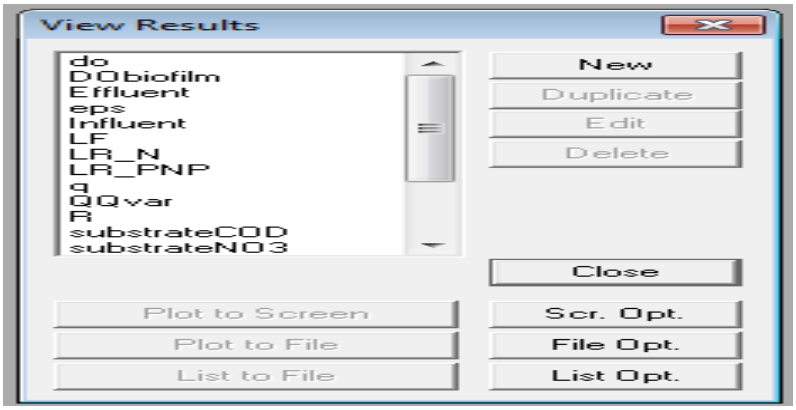

Figure 17 The AQUASIM dialog box to specify plotted graph

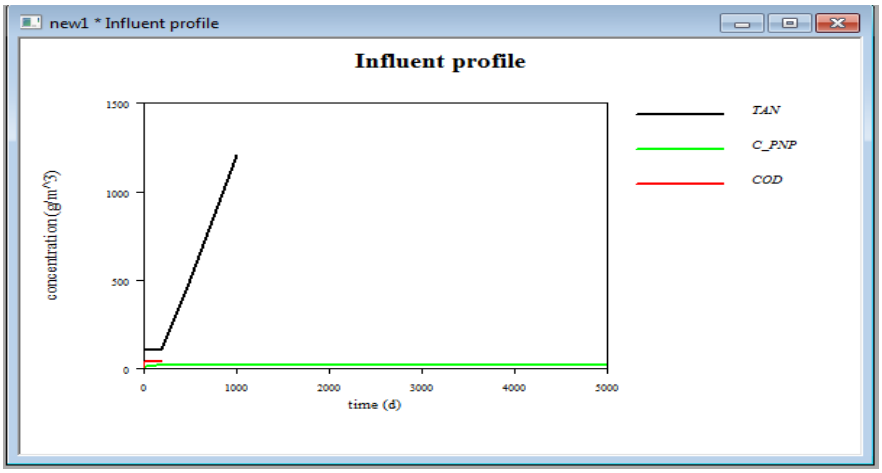

Figure 18 The AQUASIM dialog box for Influent profile graph

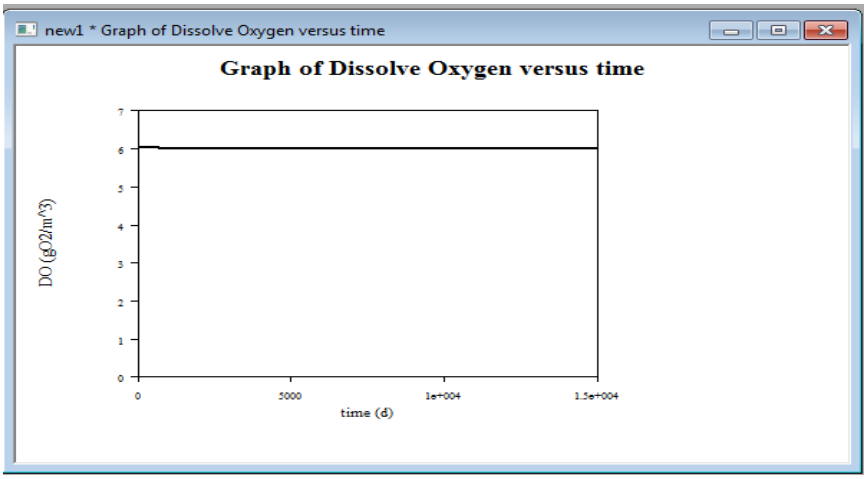

Figure 19 The AQUASIM dialog box for Dissolve Oxygen profile

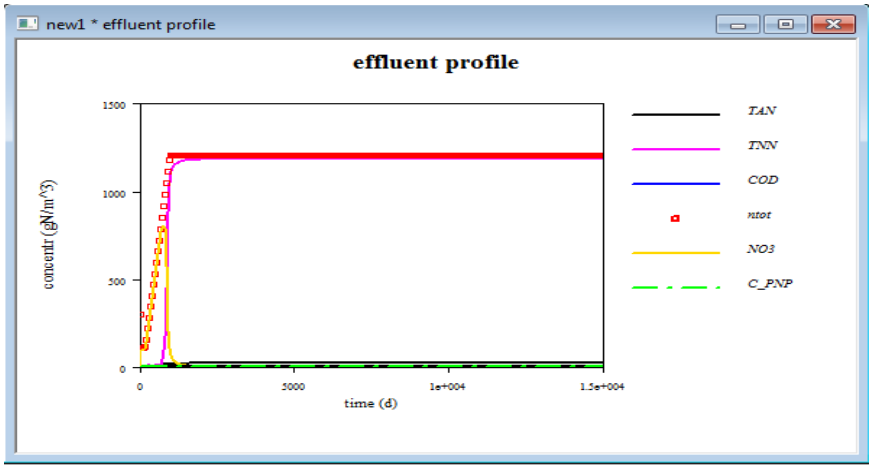

Figure 20 The AQUASIM dialog box for Effluent profile

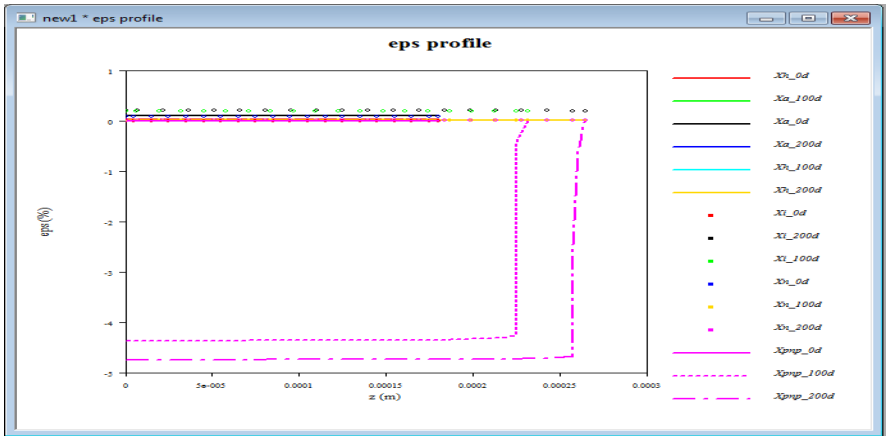

Figure 21 The AQUASIM dialog box for eps profile

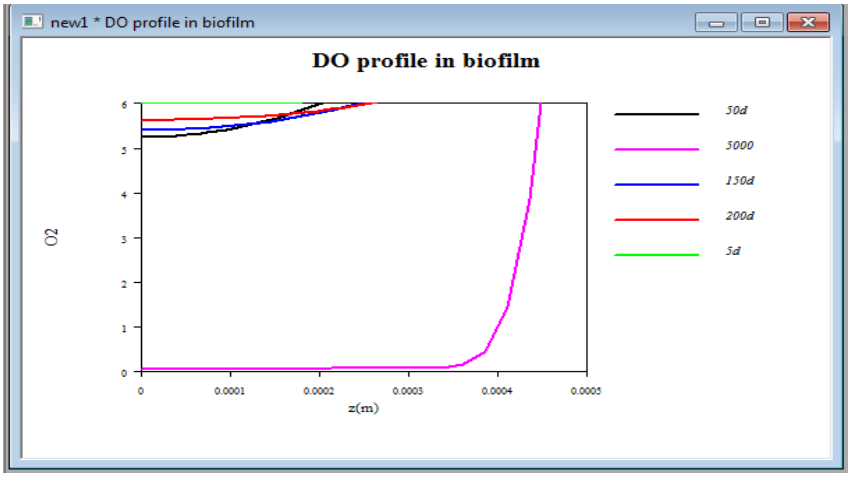

Figure 22 The AQUASIM dialog box for DO profile in biofilm

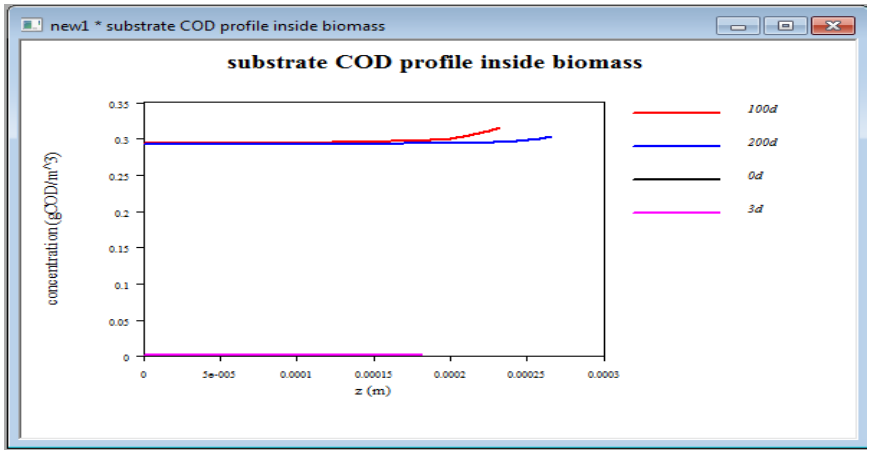

Figure 23 The AQUASIM dialog box for substrate COD profile inside biomass

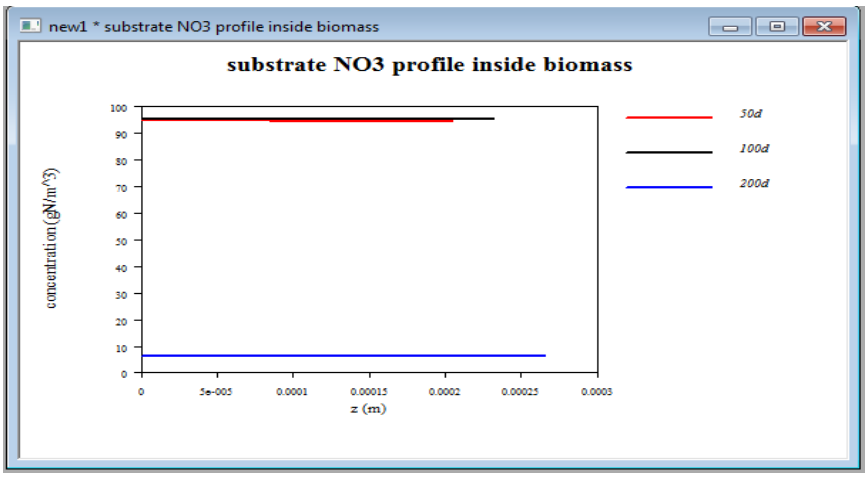

Figure 24 The AQUASIM dialog box for substrate NO3 profile inside biomas

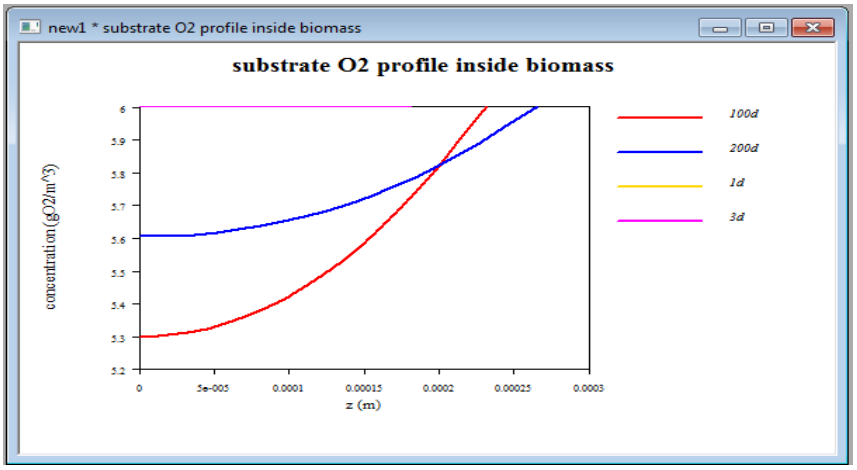

Figure 25 The AQUASIM dialog box for substrate O2 profile inside biomass

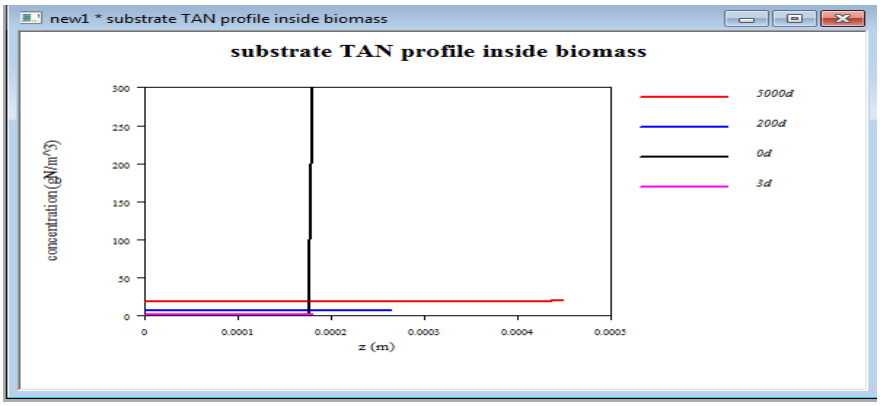

Figure 26 The AQUASIM dialog box for substrate TAN profile inside biomass

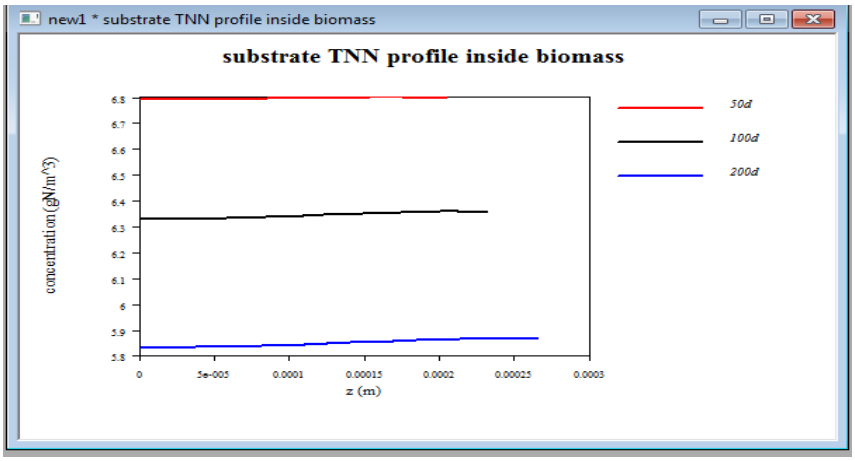

Figure 27 The AQUASIM dialog box for substrate TNN profile inside biomass

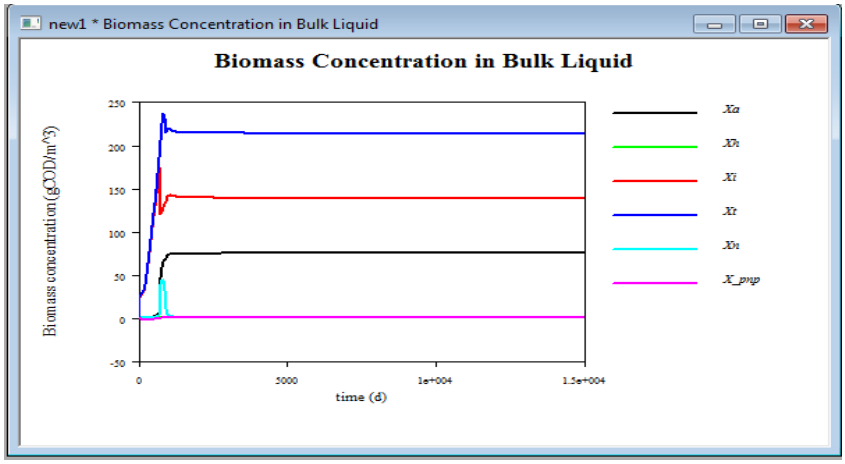

Figure 28 The AQUASIM dialog box for biomass concentration in bulk liquid